Symmetry Selection Rules for Vibrationally Inelastic Tunneling

N. Lorente* and M. Persson
Department of Applied Physics, Chalmers/Göteborg University, S-41296 Göteborg, Sweden

L. J. Lauhon and W. Ho
Laboratory of Atomic and Solid State Physics and Cornell Center for Materials Research, Cornell University, Ithaca, New York 14853
(Received 11 September 2000)

A combined experimental and theoretical study is presented for the C-D stretch mode excitation of acetylene isotopes, C_2HD and C_2D_2, on Cu(100) via inelastic electron tunneling (IET) in a scanning tunneling microscope junction. The calculated IET images using density functional theory show that the measured signal from C_2D_2 derives from the antisymmetric stretch mode. Selection rules are derived and involve the constraint imposed by the IET image on the symmetry characters of the vibrational mode and the adsorbate-induced electron states at the Fermi level.

DOI: 10.1103/PhysRevLett.86.2593 PACS numbers: 68.35.Ja, 34.50.Ez, 68.37.Ef, 73.20.Hb

Scanning tunneling microscope (STM) based inelastic electron tunneling spectroscopy (STM-IETS) [1,2] is proving to be a useful tool in the analysis of single molecules and chemical reactions on surfaces [3]. By recording the changes of conductance due to single-mode excitation, STM-IETS is capable of mapping the excitation of vibrational modes in real space [2] with sub-Å spatial resolution and meV spectral resolution. Despite the obvious promise of a spectroscopy with these figures of merit, the general applicability of STM-IETS cannot be addressed without some understanding of the underlying excitation mechanism. Inelastic excitation mechanisms and selection rules are well known for more mature techniques such as electron energy loss spectroscopy (EELS) and infrared reflection absorption spectroscopy (IRAS). Such understanding is often crucial to the analysis of experimental findings and thus very important in the analysis of STM-IETS data.

In this Letter, we report development of selection rules for STM-IETS based on the symmetry of the electronic structure and vibrational modes of acetylene chemisorbed on Cu(100). First, the spatial distribution of the C-D bond excitation via IET is carefully examined for C_2DH and C_2D_2 to permit detailed comparison with theoretical calculations. Excellent agreement is found with theoretical IET images calculated using density functional theory (DFT) in a many-body extension of Tersoff and Hamman's approach to STM image calculation. Analyses of the underlying contributions to the theoretical images based on the symmetries and energies of the relevant electronic states permit the origin of the experimental signal to be conclusively identified as the antisymmetric C-D stretch mode of DCCD. The selection rules arising from this treatment have general implications for the observability of vibrational modes using STM-IETS.

The homemade variable-temperature STM used in the acquisition of single-molecule vibrational spectra and images has been described elsewhere [1,2]. Experiments were conducted at 9 K to minimize vibrational peak widths and thermal drift in the STM junction. With the feedback off, the second derivative of the tunneling current d^2I/dV^2 was measured by a lock-in amplifier tuned to the second harmonic of a small ac bias modulation. Peaks in d^2I/dV^2 appear when the dc sample bias matches the energy of a molecular vibration. The C-D stretch modes of DCCD and HCCD appear at 266 and 269 meV, respectively. The energy of the C-H (C-D) stretch is consistent with a bent C-H bond away from the surface and the C-C bond parallel to the surface [4].

With the sample bias set to the energy of the DCCD C-D stretch, the spatial variation of d^2I/dV^2 was recorded to produce an image of the vibrational excitation [Fig. 1(a)]. Vibrational images were taken concurrently with constant current images to correlate vibrational structure with molecular position. Cross sections of Fig. 1(a) are shown in Fig. 1(b). The maximum vibrational signal occurs at the center of the molecule. Vibrational images were taken with the molecule rotated 90° from the orientation shown in Fig. 1(a) to check that the small differences in cross sections along and perpendicular to the C-C bond axis were not an artifact of the tip shape.

Vibrational images were also taken for the C-D stretch of HCCD. Cross sections of the images along the C-C bond axis are shown in Fig. 1(c) for two orientations of HCCD, 180° apart. While the source of the signal from HCCD is clearly the C-D stretch, DCCD has both symmetric (ν_{ss}) and antisymmetric stretch (ν_{as}) modes that could contribute to the experimental signal. To the extent that the C-D bonds are excited independently, one might expect the sum of the HCCD and DCCH intensity profiles to match that of DCCD. Figure 1(d) shows that, within experimental error, the two profiles are the same. In the absence of both known selection rules and known vibrational energies for the modes in question, the experiment alone cannot determine whether the DCCD signal comes from single bond excitation, or single or multiple mode excitation. To determine the physical significance of this agreement, we need to

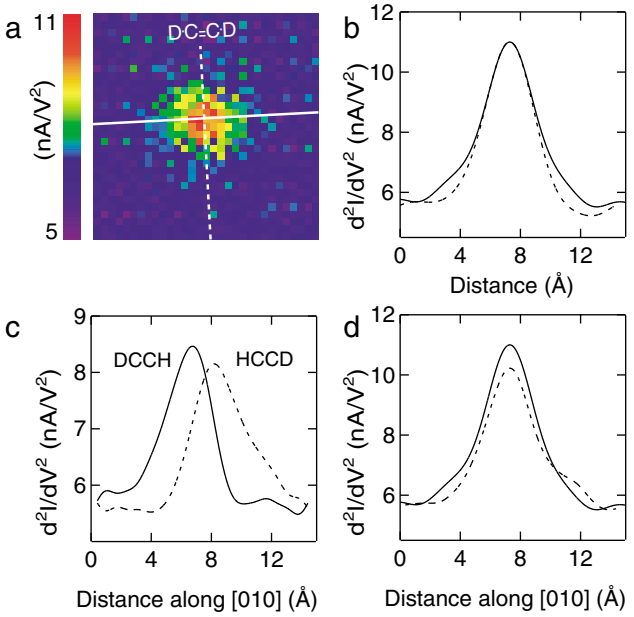

FIG. 1 (color). Vibrational microscopy of DCCD. (a) 14 × 14 Å^2 spatial map of d^2I/dV^2 at the energy of the C-D stretch mode (266 meV) showing localized excitation of the molecular vibration. To improve the signal to noise ratio, the image is an average of four separate scans. The solid line contains the C-C bond axis along the [010] direction and the dashed line is along the [001] direction. (b) Smoothed cross sections of (a) taken along the [010] (solid line) and [001] (dashed line) directions. (c) Smoothed cross sections of the C-D stretch vibrational microscopy images taken along the C-C axis for the two possible orientations of HCCD, 180° apart. (d) Sum of the profiles of (c) (dashed line) compared with the cross section of DCCD taken along the C-C axis (solid line). The dashed line has been offset -5.5 nA/V^2 to avoid double counting the background in the sum. The vibrational images were taken under the following conditions: tunneling gap set point of 0.5 nA and 266 mV; 10 mV rms modulation at 384 Hz; 200 ms dwell time per data point; a 0.5 Å pixel resolution. For HCCD, the tunnel gap was set at a bias of 269 mV.

understand the origin of the inelastic images and what information about the excitation process can be obtained from them.

We have recently developed a theory of STM-IETS that can explain the experimental vibrational microscopy images [5]. This theory generalizes the approach by Tersoff and Hamman [6] for tunneling in the STM by including perturbatively the effects of the electron-vibration coupling in the sample on the tunneling conductance. The differential conductance, dI/dV, is proportional to the local electron density of states, $\rho(\mathbf{r}_0, \epsilon_F + eV)$, at the position $\mathbf{r}_0$ of the tip apex, which is found to have a discontinuity, $\Delta\rho(\mathbf{r}_0)$, at the bias V corresponding to the vibrational energy $\hbar\Omega$ of a mode. The relative change in differential conductance, η_{tot}, is then given by

$$\eta_{\mathrm{tot}}(\mathbf{r}_0) = \frac{\Delta\rho(\mathbf{r}_0)}{\rho(\mathbf{r}_0, \epsilon_F)}, \tag{1}$$

where η_{tot} can be decomposed into an inelastic term, η_{ine}, and an elastic term, η_{ela} as [7,8],

$$\eta_{\mathrm{tot}}(\mathbf{r}_0) = \eta_{\mathrm{ine}}(\mathbf{r}_0) + \eta_{\mathrm{ela}}(\mathbf{r}_0). \tag{2}$$

To leading order in electron-vibration coupling these two terms are given by

$$\eta_{\mathrm{ine}}(\mathbf{r}_0) = \frac{1}{\rho(\mathbf{r}_0, \epsilon_F)} \times \sum_\mu \left| \sum_\lambda \frac{\langle\psi_\mu|\delta v|\psi_\lambda\rangle\langle\psi_\lambda|\mathbf{r}_0\rangle}{\epsilon_\lambda - \epsilon_\mu + i0^+} \right|^2 \delta(\epsilon_F - \epsilon_\mu), \tag{3}$$

and

$$\eta_{\mathrm{ela}}(\mathbf{r}_0) = \frac{-2\pi^2}{\rho(\mathbf{r}_0, \epsilon_F)} \times \sum_\mu \left| \sum_\lambda \langle\psi_\mu|\delta v|\psi_\lambda\rangle\langle\psi_\lambda|\mathbf{r}_0\rangle \delta(\epsilon_\mu - \epsilon_\lambda) \right|^2 \times \delta(\epsilon_F - \epsilon_\mu). \tag{4}$$

Here we have taken the quasistatic limit, $\hbar\Omega \to 0$. $|\psi_\lambda\rangle$ is an intermediate one-electron state in the sample with energy ϵ_λ, which couples through the deformation potential, $\delta v(\mathbf{x}) = \sqrt{\frac{\hbar}{2M\Omega}}\frac{\partial v}{\partial Q}(\mathbf{x}, 0)$, to a final one-electron state in the sample, $|\psi_\mu\rangle$, with energy ϵ_μ. $v(\mathbf{x}, Q)$ is the effective one-electron potential as a function of the normal coordinate Q of the vibrational mode with mass M. The one-electron wave functions, energies, and potentials are obtained from density functional theory using plane wave pseudopotential calculations [5,9,11].

In the present work, we have studied the STM-IETS signals of the C-D stretch modes of DCCD and HCCD on Cu(100). As described elsewhere [5], the bonding geometry and vibrational energies of this system are well described by our density functional calculations [9]. The calculated energies of the ν_{as} and ν_{ss} modes in DCCD are 275 and 281 meV, respectively. The calculated C-D stretch of HCCD at 278 meV is 3 meV higher than the ν_{as} mode of DCCD, and the experimental C-D stretch of HCCD is 3 meV higher than the experimental C-D stretch of DCCD. This comparison suggests that the STM-IETS signal for DCCD originates from excitation of the ν_{as} mode.

In Fig. 2 we present the theoretical vibrational microscopy images, $\eta_{\mathrm{tot}}(\mathbf{r}_0)$, of the C-D stretch modes of DCCD and HCCD. The profiles of $\eta_{\mathrm{tot}}(\mathbf{r}_0)$ along the C-C axis in Fig. 2(c) for the ν_{as} and ν_{ss} modes show directly that the dominant signal comes from the ν_{as} mode. The signal from the ν_{ss} mode has two maxima at the C-D bonds of 1.4% (1.2% at the center of the molecule) whereas the signal from the ν_{as} mode has its maximum of 9.6% at the center of the molecule. Both the image [Fig. 2(a)] and the inelastic profiles [Fig. 2(b)] of the signal are in excellent agreement with the experimental results in Figs. 1(a) and 1(b) for the ν_{as} mode; the experiment gives a maximum value of 8 ± 1%. The same level of agreement between theory and experiment is obtained for the corresponding IET signal for the C-D stretch in HCCD, Fig. 1(c) compared to Fig. 2(c) and also shown earlier by Lorente and

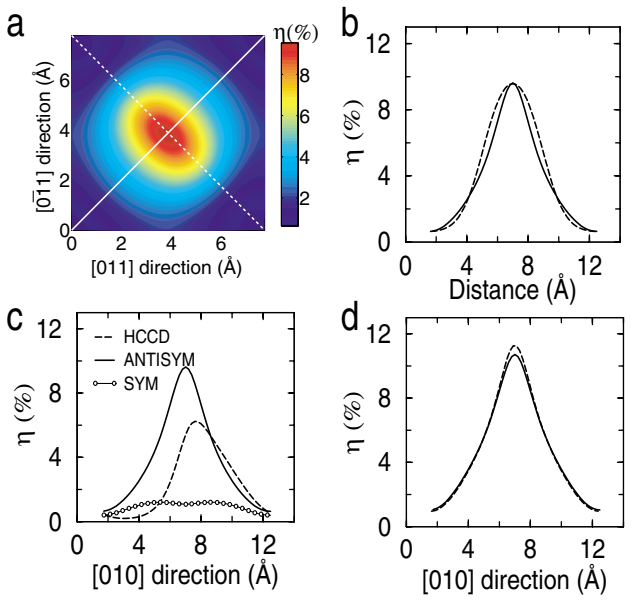

FIG. 2 (color). Theoretical spatial dependence of the C-D stretch intensity. (a) Inelastic efficiencies for the antisymmetric C-D stretch stretch mode of C_2D_2 over the 3×3 supercell of Cu(100), 7.5×7.5 Å. The C-C axis is oriented along the [010] direction, represented in the figure as a solid line. (b) Inelastic profiles along the [010] direction (full line) and [001] direction (dashed line) as depicted in (a). (c) Profiles of the inelastic efficiency along the C-C axis for the antisymmetric and symmetric modes of DCCD, and the C-D stretch of HCCD. (d) Inelastic profile (full line) along the C-C axis for the sum of the antisymmetric and symmetric modes compared with the sum of the inelastic efficiency of two independent C-D stretch modes corresponding to the two bonds of DCCD (dashed line).

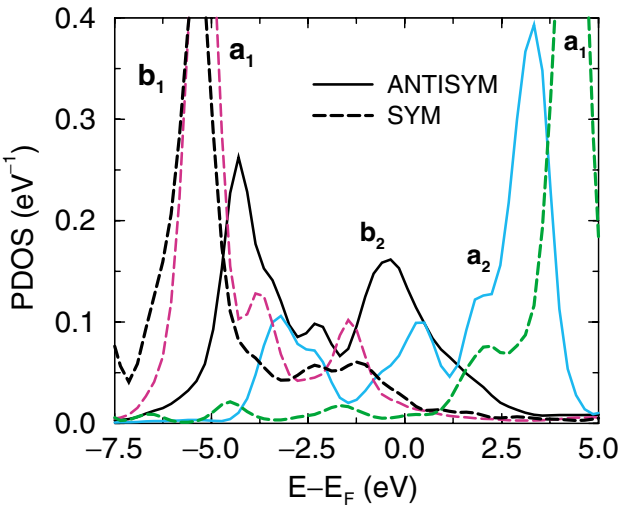

FIG. 3 (color). Projected density of states (PDOS) of acetylene chemisorbed on Cu(100). The projections are on molecular orbitals of the free bent molecule. The PDOS are classified both according to the symmetry labels of the molecular orbitals with respect to the symmetry group, C_{2v}, of the adsorption site and the symmetry with respect to the plane σ_v perpendicular to the C-C axis. The molecular orbitals are derived from the bonding π (b_1 and a_1) and the antibonding π^* (b_2 and a_2) orbitals and the antibonding C-D orbital (a_1) of the free linear molecule [12].

Persson [5]. Thus this analysis of the theoretical images of the IETS signal for DCCD allows us to conclude that the detected IETS signal originates from the antisymmetric mode, as was suggested from the analysis of the vibrational energies.

The dominance of the ν_{as} mode in IETS of DCCD may be understood by examining the symmetry of the electronic states which are coupled by the vibrational excitation. The vibration couples final states, $|\psi_\mu\rangle$, at the Fermi level, ϵ_F, with intermediate states, $|\psi_\lambda\rangle$, through the matrix element $\langle\psi_\mu|\delta v|\psi_\lambda\rangle$ of the deformation potential, $\delta v(\mathbf{x})$ in Eqs. (3) and (4). In general, $\delta v(\mathbf{x})$ is expected to be short ranged so that the molecular orbitals, $\psi_a(\mathbf{x})$, of the free molecule form a local basis set, that is, $\langle\psi_\mu|\delta v|\psi_\lambda\rangle \approx \sum_a \langle\psi_\mu|\psi_a\rangle\langle\psi_a|\delta v|\psi_\lambda\rangle$, suggesting that the relevant final states ψ_μ are those states at ϵ_F having a large overlap $\langle\psi_\mu|\psi_a\rangle$. In Fig. 3 we show the density of states of the molecule-surface system projected on $|\psi_a\rangle$ of the bent free molecule. We have classified $|\psi_a\rangle$ according to their symmetry with respect to the mirror plane (σ_v) perpendicular to the molecular C-C axis. The density of states at ϵ_F has a dominant antisymmetric character with respect to σ_v, which can be traced back to the b_2 state of the bent molecule. The a_2 and b_2 states of the free bent molecule are derived from the π^* orbitals of the linear molecule [12].

The symmetry of the IET image is determined by the symmetry characters of the deformation potential and the projected density of states (PDOS) at ϵ_F. The IET image is built up by the intermediate states $|\psi_\lambda\rangle$ and the matrix element $\langle\psi_a|\delta v|\psi_\lambda\rangle$ is nonzero if $\psi_a^*(\mathbf{x})\delta v(\mathbf{x})\psi_\lambda(\mathbf{x})$ is totally symmetric. The symmetry character of $\delta v(\mathbf{x})$ is determined by the character of the vibrational mode; a symmetric mode with respect to a mirror plane results in a symmetric deformation potential, whereas an antisymmetric mode results in an antisymmetric deformation potential [13]. Thus we can state the following symmetry selection rule for the STM vibrational image [14]: *the IET signal has a nodal plane at a mirror plane (i.e., $|\psi_\lambda\rangle$ are antisymmetric) if the character of the projected density of states on orbitals of the free molecule is antisymmetric at ϵ_F for a symmetric stretch mode or symmetric for an antisymmetric stretch mode.*

The proposed symmetry selection rule is supported by the images of the C-D stretch modes of DCCD. Because of the predominantly antisymmetric character of the PDOS with respect to σ_v at ϵ_F, excitation of the ν_{as} mode results in an IET image with no nodal plane whereas excitation of the ν_{ss} mode is suppressed along σ_v. This argument explains why the signal at the center of the molecule is dominated by the ν_{as} mode. The proposed selection rule also explains the observed symmetry of the IET image for the frustrated rotational mode of CO on Cu(100) [15] and the O-O and O_2-Ag stretch vibrations of O_2 on Ag(110) [16]. A nodal plane was observed in the IET images for the O_2 vibrations.

The symmetries of the PDOS at ϵ_F and the vibrational modes also influence the relative magnitude of the elastic

contribution η_{ela} to the IET signal. For the ν_{ss} and ν_{as} modes at the center of the molecule, η_{ela} is -0.2% and -0.03%, respectively, which are negligible compared to the corresponding inelastic contributions η_{ine} of 1.4% and 9.6%. $|\eta_{\text{ela}}^{ss}|$ is larger than $|\eta_{\text{ela}}^{as}|$ because the elastic contribution in Eq. (4) involves only states $|\psi_\mu\rangle$ and $|\psi_\lambda\rangle$ at ϵ_F. The dominant antisymmetric character of the PDOS at ϵ_F suggests that the contribution from $\langle\psi_\mu|\delta v|\psi_\lambda\rangle$ will be appreciable only for the ν_{ss} mode.

The experimental observation that the sum of the IET signals for the C-D stretches of HCCD and DCCH reproduces the signal for the C-D stretch mode of DCCD has a simple origin. The displacement fields of the C-D stretch modes are highly localized to the D atoms so that the displacement fields of the ν_{ss} and ν_{as} modes of DCCD are well represented by symmetric and antisymmetric linear combinations of the localized displacements L and R of the D atoms in DCCH and HCCD, respectively. This form for the displacement fields gives directly the following relationship among the corresponding deformation potentials,

$$\delta v_{ss,as}(\mathbf{x}) = \frac{1}{\sqrt{2}}[\delta v_L(\mathbf{x}) \pm \delta v_R(\mathbf{x})], \tag{5}$$

where the subscripts ss and as correspond to the plus and minus sign in the linear combination of the deformation potentials for the localized modes. By substituting the relation between the deformation potentials into Eq. (3) we obtain

$$\eta_{\text{ine}}^{ss,as}(\mathbf{r}_0) = \frac{1}{2}\Big[\eta_{\text{ine}}^{L}(\mathbf{r}_0) + \eta_{\text{ine}}^{R}(\mathbf{r}_0) \pm \frac{2}{\rho(\mathbf{r}_0)} \times \sum_{\mu,\nu,\lambda} \frac{\langle\mathbf{r}_0|\nu\rangle\langle\lambda|\mathbf{r}_0\rangle}{(\epsilon_\mu - \epsilon_\lambda - i0^+)(\epsilon_\mu - \epsilon_\nu + i0^+)} \times \langle\lambda|v_L|\mu\rangle\langle\mu|v_R|\nu\rangle\delta(\epsilon_F - \epsilon_\mu)\Big], \tag{6}$$

where ss and as have the same correspondence to the signs of the cross term as in Eq. (5). Such a cross term also appears for $\eta_{\text{ela}}^{ss,as}(\mathbf{r}_0)$ in Eq. (4) and the cross terms cancel when the contributions from ν_{ss} and ν_{as} are added. Thus, we find that

$$\eta_{\text{tot}}^{ss}(\mathbf{r}_0) + \eta_{\text{tot}}^{as}(\mathbf{r}_0) = \eta_{\text{tot}}^{L}(\mathbf{r}_0) + \eta_{\text{tot}}^{R}(\mathbf{r}_0). \tag{7}$$

This result is essentially a consequence of perturbation theory resulting in a quadratic dependence of $\eta_{\text{tot}}(\mathbf{r}_0)$ on the deformation potential and can be easily generalized and extended. Since $\eta_{\text{tot}}^{as}(\mathbf{r}_0)$ dominates $\eta_{\text{tot}}^{ss}(\mathbf{r}_0)$, the IET signal for the observed C-D stretch mode in DCCD is essentially given by the sum of the signals from the C-D stretch modes of DCCH and HCCD. This result is consistent with our finding that the ν_{as} mode dominates the observed signal.

In addition, the calculations show that the measured IET signal from C_2D_2 derives from the antisymmetric mode and that the observed matching of the sum of the IET intensity profiles of HCC-D and D-CCH modes to the profile of D-CC-D mode has a simple origin. The much larger IET intensity for the antisymmetric mode than for the symmetric mode at the center of the molecule can be understood in terms of restrictions imposed by the symmetry characters of the vibrational mode and the projected density of states at the Fermi level. The proposed symmetry selection rule is expected to provide an understanding of the single molecule vibrational intensity and its spatial symmetry as measured by STM-IETS.

M. P. and N. L. acknowledge support by the European Union TMR project "Atomic/Molecular Manipulation" and the Swedish Natural Science Research Council (NFR). The assistance and computer resources provided by UNICC at Chalmers and PDC in Stockholm have been indispensable. The Cornell effort was funded by the National Science Foundation under Grant No. DMR-9417866.

*Permanent address: Laboratoire Collisions Agrégats Réactivité, UMR 5589, IRSAMC. Université Paul Sabatier, 31062 Toulouse Cedex, France.

[1] B. C. Stipe, M. A. Rezaei, and W. Ho, Science **280**, 1732 (1998); Rev. Sci. Instrum. **70**, 137 (1999).
[2] B. C. Stipe, M. A. Rezaei, and W. Ho, Phys. Rev. Lett. **82**, 1724 (1999).
[3] L. J. Lauhon and W. Ho, Phys. Rev. Lett. **84**, 1527 (2000).
[4] X. F. Hu, C. J. Chen, and J. C. Tang, Surf. Sci. **365**, 319 (1996).
[5] N. Lorente and M. Persson, Phys. Rev. Lett. **85**, 2997 (2000).
[6] J. Tersoff and D. R. Hamann, Phys. Rev. Lett. **50**, 1998 (1983); Phys. Rev. B **31**, 805 (1985).
[7] C. Caroli, R. Combescot, P. Nozières, and D. Saint-James, J. Phys. C **5**, 21 (1972).
[8] B. N. J. Persson and A. Baratoff, Phys. Rev. Lett. **59**, 339 (1987).
[9] We used the code DACAPO-1.30 of CAMP, DTH, Denmark, and the exchange and correlation effects were described by the generalized gradient approximation of Perdew and co-workers [10]. The scattering from the ion cores was represented by ultrasoft pseudopotentials and the wave functions were expanded in plane waves with a kinetic energy cutoff at 30 Ry. The vibrational frequencies and displacement fields were obtained by solving the dynamical matrix that was calculated from forces in displaced configurations.
[10] J. P. Perdew *et al.,* Phys. Rev. B **46**, 6671 (1992).
[11] N. Lorente, L. Bengtsson, and M. Persson (to be published).
[12] D. M. Hoffman, R. Hoffmann, and C. R. Fisel, J. Am. Chem. Soc. **104**, 3858 (1982).
[13] L. D. Landau and E. M. Liftschitz, *Quantum Mechanics* (Pergamon Press, Oxford, 1977), p. 406.
[14] The selection rule was derived using the Tersoff-Hamann approximation of an s wave tip but is valid as long as the tunneling-active tip wave functions are totally symmetric. This rule can be straightforwardly generalized to account for other symmetry characters of these wave functions.
[15] L. J. Lauhon and W. Ho, Phys. Rev. B **60**, R8525 (1999).
[16] J. R. Hahn, H. J. Lee, and W. Ho, Phys. Rev. Lett. **85**, 1914 (2000).